

## ANALYSIS OF CONFINEMENT LOSS AND BIREFRINGENCE IN HEXAGONAL AND OCTAGONAL PCF DUE TO EXTERNAL STRESS

M. R. Khatun<sup>1</sup> and M. S. Islam<sup>2</sup>

<sup>1,2</sup>Institute of Information and Communication Technology,  
Bangladesh University of Engineering and Technology, Dhaka-1000, Bangladesh  
<sup>1</sup>rokeya.alam@yahoo.com, <sup>2</sup>mdsaifulislam@iict.buet.ac.bd

***Abstract-**In this paper, we have analyzed external stress induced birefringence and confinement loss properties for hexagonal and octagonal air hole arranged PCFs (photonic crystal fibers). Here finite element method (FEM) has been used for stress and optical analysis in COMSOL Multiphysics environment. The analysis has been carried out on both types of structures by varying air hole diameter. Different stress has been applied on the PCFs boundary and the effective indices, birefringence and confinement loss are calculated as a function of stress. It is found that birefringence and confinement loss properties of hexagonal PCFs are more sensitive than octagonal. Again this effect is larger for PCFs with smaller air hole diameters than larger.*

**Keywords:** Photonic crystal fiber (PCF), finite element method (FEM), elasto-optic effect, birefringence and confinement loss.

### 1. INTRODUCTION

Photonic crystal fibers (PCFs) are a new class of optical fibers. PCFs also known as microstructured fibers that has arrays of holes running along its length. Microstructured fibers guide light due to modified total internal reflection. Unlike conventional fibers, PCFs can be made entirely from a single material, typically undoped silica [1]. The holes act to lower the effective refractive index in the cladding region and so light are confined to the solid core, which has a relatively higher index. In a PCF, the number of holes and their sizes, shapes, orientations and placements can provide degrees of freedom and hence unique properties, which are not available in conventional optical fibers [2-3]. The strong wavelength dependency of the effective refractive index and the inherently large design flexibility of the PCFs allow for a whole new range of novel properties [4-5]. Such properties include endlessly single-moded fibers, extremely nonlinear fibers and fibers with anomalous dispersion in the visible wavelength region. Propagation properties of PCFs have been investigated widely using different analysis techniques and tools [6-8]. From some recent research works we find that hydrostatic pressure, axial force, twisting and elongation may cause changes in fiber structure and properties, when they are used as sensor for civil structures or acoustic pressure in underwater and underground communication systems [9-12]. But few works has been done to understand the external stress effects on PCFs. These research works mainly carried out on effective index, birefringence, polarization mode dispersion and confinement loss properties only for hexagonal air-holes

arranged PCFs with few design parameters. In this research work an analysis has been carried out to observe the effect of thermal and external stress on birefringence and confinement loss for both hexagonal and octagonal air hole arranged PCFs. The fiber designs have been carried out for both types of PCFs by varying air hole diameter. Then different stress has been applied on the PCFs boundary and the effective indices, birefringence and confinement loss are calculated as a function of stress. It is found that the external stress induces higher birefringence for hexagonal PCF than octagonal. It also found that confinement loss as a function of stress increases more sharply for hexagonal PCF than octagonal. For both structures effect of stress on confinement is lower for larger air diameter than smaller.

### 2. FORMULATION

To study the distribution of stresses in an optical fiber, the finite element approach is a highly suitable method to be applied due to its flexibility and power. In optical fibers or waveguides under stress, the original refractive index of the material changes due to photoelastic effect. The new refractive index for x and y polarized light can be calculated from the following equation [6]:

$$n_x = n_0 + C_1\sigma_x + C_2(\sigma_y + \sigma_z) \quad (1.1)$$

$$n_y = n_0 + C_1\sigma_y + C_2(\sigma_x + \sigma_z) \quad (1.2)$$

$$n_z = n_0 + C_1\sigma_z + C_2(\sigma_x + \sigma_y) \quad (1.3)$$

where,  $C_1, C_2$  are the elasto-optic coefficient of the fiber

or waveguide material,  $n_{x0}$ ,  $n_{y0}$  and  $n_{z0}$  are the unstressed refractive indices of the material and  $n_x$ ,  $n_y$  and  $n_z$  are the main diagonal element of the anisotropic refractive index tensor.

PML is an absorbing layer specially studied to absorb without reflection the electromagnetic waves [7]. Using this layer, we can estimate the confinement loss of any optical fiber. To define a PML, an additional modeling domain (sub domain) outside the boundaries is added to absorb the leaked light. The PML can have arbitrary thickness and is specified to be made of an artificial absorbing material. The material has nisotropic permittivity and permeability that match the permittivity and permeability of the physical medium outside the PML in such a way that there are no reflections.

An eigenvalue equation for the magnetic field  $H$  is derived from Helmholtz equation

$$\nabla \times (\varepsilon^{-1} \nabla \times H) - k_0^2 \mu H = 0 \quad (2)$$

where, permeability,  $\mu = \mu_0 \mu_r L$

permittivity,  $\varepsilon = \varepsilon_0 \varepsilon_r L$

propagation constant,  $k_0 = 2\pi / \lambda$ .

For a PML that is parallel to one of the Cartesian coordinate planes,  $L$  becomes diagonal

$$L = \begin{bmatrix} L_{xx} & 0 & 0 \\ 0 & L_{yy} & 0 \\ 0 & 0 & L_{zz} \end{bmatrix} \quad (3)$$

where,

$$L_{xx} = \frac{s_y s_z}{s_x}, \quad L_{yy} = \frac{s_x s_z}{s_y}, \quad L_{zz} = \frac{s_x s_y}{s_z}.$$

The parameters  $s_x$ ,  $s_y$ , and  $s_z$  are the complex-valued coordinate scaling parameters. By assigning suitable values to these, it can be obtained a PML that absorbs waves traveling in a particular direction. The values below represent a PML that attenuates a wave traveling in the  $x$  direction.

$$s_x = a - bi, \quad s_y = 1, \quad s_z = 1$$

where,  $a$  and  $b$  are arbitrary positive real numbers.

Optical analysis is performed for calculating the effective mode indices for different modes propagating within the fiber. It involves dealing with perpendicular hybrid mode waves. The mode analysis is made on a cross-section in the  $x$ - $y$  plane of the fiber.

The wave propagates in the  $z$  direction has the form

$$H(x, y, z, t) = H(x, y) e^{j(\omega t - \beta z)} \quad (4)$$

where  $\omega$  is the angular frequency and  $\beta$  the propagation constant. An eigenvalue equation for the magnetic field  $H$  is derived from Helmholtz equation in the fiber cross section reduces to:

$$\nabla \times ([n]^{-2} \nabla \times H) - k_0^2 H = 0 \quad (5)$$

which is solved for the eigenvalue of  $-\beta^2$ .

Boundary condition along the outside of the cladding the magnetic field is set to zero. Because the amplitude of the field decays rapidly as a function of the radius of the cladding this is a valid boundary condition. This condition is expressed by the equation:

$$n \times H = 0 \quad (6)$$

For a confined mode there is no energy flow in the radial direction, thus the wave must be evanescent in the radial direction in the cladding. Effective mode index of a confined mode,

$$n_{eff} = \frac{\beta}{k_0}. \quad (7)$$

This is true only if  $n_{Clad} < n_{eff} < n_{Core}$ . The effective index  $n_{eff}$  of the fundamental mode of the PCF is computed as a function of wavelength. Then the modal birefringence of the fiber is obtained by

$$B_m = n_{eff}^x - n_{eff}^y \quad (8)$$

where,  $n_{eff}^x$  and  $n_{eff}^y$  are the effective indices in  $x$  and  $y$  direction respectively.

The effective index ( $n_{eff}$ ) found here is a complex number and the real part,  $\text{Re}(n_{eff})$  is used to calculate dispersion and the imaginary part,  $\text{Im}(n_{eff})$  is used for confinement loss calculation.

$$\text{Confinement loss} = \frac{40\pi \cdot \text{Im}(n_{eff}) \times 10^6}{\lambda \ln(10)} \quad (9)$$

### 3. RESULTS AND DISCUSSION

We have analyzed external stress-induced characteristics of birefringence and confinement loss in PCFs using the finite-element method (FEM). COMSOL Multiphysics has been used here as a modeling and simulation tool, where a combination of structural mechanics module and electromagnetic module has been used to carry out the stress analysis and optical mode analysis of the PCFs respectively.

We considered two types of PCFs.

- Hexagonal PCF (the structures are designed by hexagonal air hole arrangement).
- Octagonal PCF (the structures are designed by octagonal air hole arrangement).

PCFs are made by only single material ( $\text{SiO}_2$ ), where  $n_s=1.45$ . Operating wave length is  $1.55 \mu\text{m}$ . External stresses  $P$  is considered from  $0\text{Pa}$  to  $5\text{GPa}$ . Here  $D$  is cross sectional diameter,  $d$  is the air-hole diameter  $\Lambda$  is pitch (distance between two air holes),  $e$  is PML width and  $N_r$  is the number of air hole rings. For both structures initially the dimension of the structure is-  $D= 12.0 \mu\text{m}$ ,  $\Lambda = 2.5 \mu\text{m}$ ,  $N_r = 4$ ,  $e = 1 \mu\text{m}$  and  $d = 1.2 \mu\text{m}$ , which is shown in Fig.1. Other designs are made by varying only

air hole diameter (0.8  $\mu\text{m}$ , 1.0  $\mu\text{m}$ , 1.2  $\mu\text{m}$ , 1.4  $\mu\text{m}$  and 1.6  $\mu\text{m}$ ) for both hexagonal and octagonal PCFs.

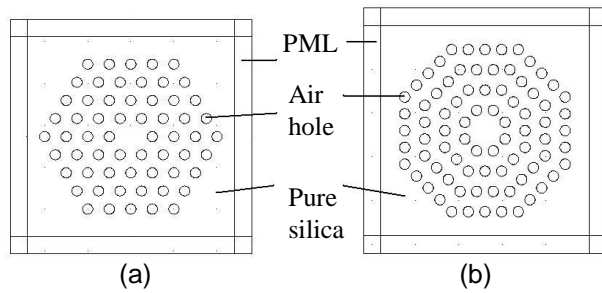


Fig.1: Cross sections of PCFs (a) Hexagonal lattice, (b) Octagonal lattice.

Here finite external stress is applied on boundary from all direction. This causes stress distribution over the fiber cross section. Fig.2 shows arrow displacement under external stress for hexagonal air hole arrangement, where the arrow direction shows pressure is applied uniformly from all directions. The power flow for the fundamental  $x$  polarized mode is shown in Fig.3.

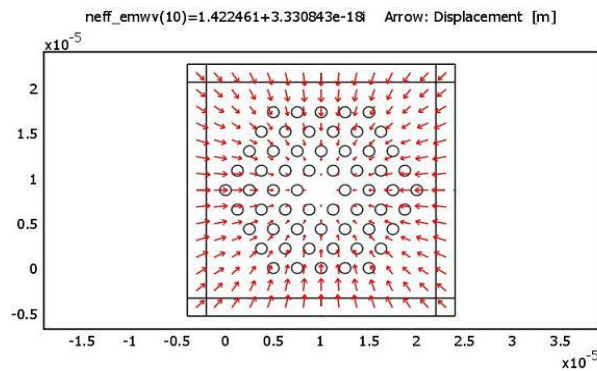


Fig.2: Arrow displacement under external stress for hexagonal air hole arrangement with external stress 5GPa, where  $d=1.2\mu\text{m}$ ,  $\Lambda=2.5\mu\text{m}$ ,  $e=1\mu\text{m}$  and  $Nr=4$ .

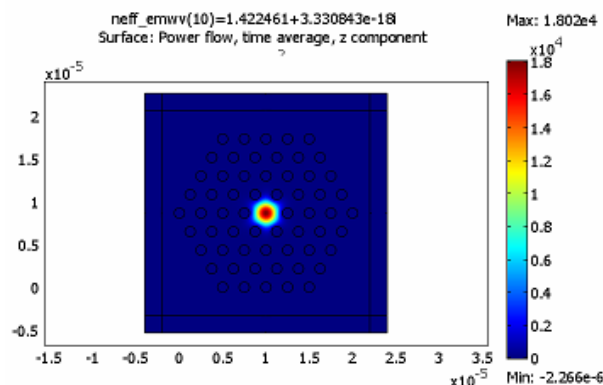


Fig.3: Power flow, time average,  $z$  component hexagonal air hole arrangement with external stress.

### 3.1 Effective Index

To get the stress effect on PCF we must perform the stress analysis before optical analysis because the stress-induced corrections of the refractive index are

used as input information for optical analysis by FEM. We have got the modal effective index as the output of optical analysis. The external stress acting on the holey fiber induces a specific stress distribution in the fiber's cross section and makes deformation of the fiber's structure. Amount of deformation is different for different structured PCFs. So that the stress induced effective index for hexagonal and octagonal PCFs are not same. The Fig.4 shows that effective index changes more sharply for hexagonal structure than octagonal with the increase of stress that agrees with the result found in [9]. To compare the result here we considered same design and operating parameters for both types of PCFs.

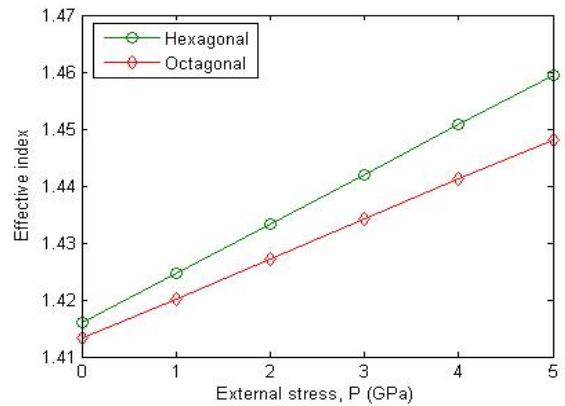


Fig.4: External stress effect on effective index for both hexagonal and octagonal air hole arrangement, where  $\lambda=1.55\mu\text{m}$ ,  $d=1.6\mu\text{m}$ ,  $\Lambda=2.5\mu\text{m}$  and  $Nr=4$ .

### 3.2 Birefringence

Stress distribution in the fiber's cross section and deformation of the fiber's structure both factor induces different modal effective index in both axis ( $x$  and  $y$ ), which causes modal birefringence. So stress induced birefringence is also different for hexagonal and octagonal PCFs.

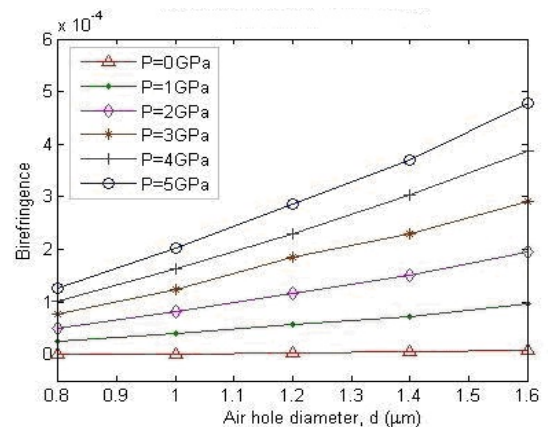


Fig.5: Birefringence of hexagonal PCF as a function of air hole diameter and external stress, where  $\lambda=1.55\mu\text{m}$ ,  $\Lambda=2.5\mu\text{m}$  and  $Nr=4$ .

Fig.5 shows that birefringence increases almost linearly as a function of air hole diameter for hexagonal PCF with fixed pitch  $\Lambda=2.5\mu\text{m}$ . It also depicts that

birefringence increases with the increase of external stress that agrees with the result found in [9-11]. Similarly Fig.6 shows the birefringence as a function of air hole diameter for octagonal PCF under external stress. Here also birefringence increases with the increase of stress. But the effect is sharper for hexagonal air arrangement PCF than octagonal. This is shown in Fig.7 where the design and operating parameters are same for both structures.

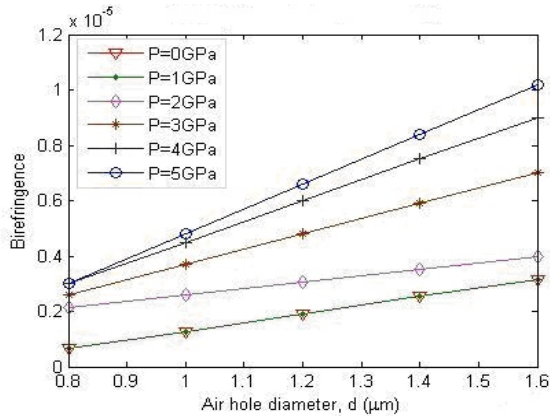


Fig.6: Birefringence of octagonal PCF as a function of air hole diameter and external stress, where  $\lambda=1.55\mu\text{m}$ ,  $\Lambda=2.5\mu\text{m}$  and  $Nr=4$ .

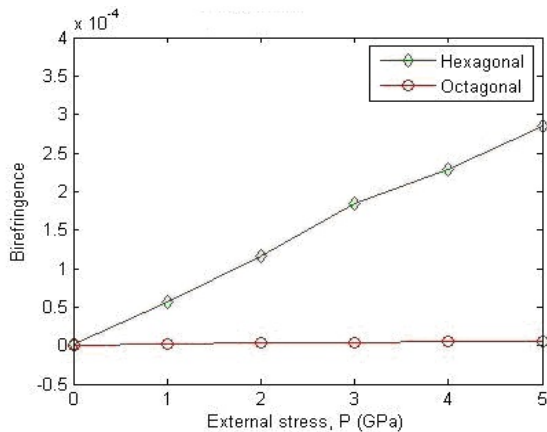


Fig.7: External stress induced birefringence for both hexagonal and octagonal PCF, where  $\lambda=1.55\mu\text{m}$ ,  $d=1.6\mu\text{m}$ ,  $\Lambda=2.5\mu\text{m}$  and  $Nr=4$ .

### 3.3 Confinement Loss

All the PCF guided modes are leaky. In solid-core PCFs light is confined within a core region by the air-holes. Light will move away from the core if the confinement provided by the air-holes is inadequate. Because of the finite transverse extent of the confining structure, the effective index is a complex value; its imaginary part is related to losses. Due to external stress deformation of the fiber's structure causes confinement loss. Fig.8 and Fig9 shows the variation of confinement loss against external stress for hexagonal and octagonal air hole arrangement PCFs respectively. From the figures it is clear that confinement loss gradually decreases with the increase of air hole diameter for both structures that agrees with the result found in [12]. It also shows that

confinement loss is very high for larger external stress with smaller air hole diameter ( $d=0.8\mu\text{m}$  to  $d=1.0\mu\text{m}$ ). Again, Fig.10 (a) and (b) shows the result of confinement loss as a function of external stress for both hexagonal and octagonal PCFs, where we considered same design and operating parameters. The figures show that stress effect on confinement loss is larger on hexagonal structure than octagonal and this effect gradually decreases for larger air hole diameter.

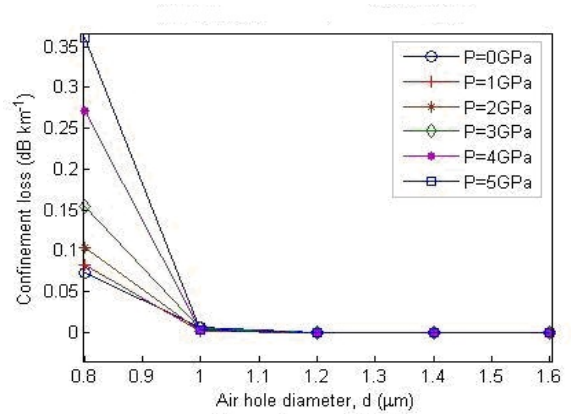


Fig.8: Confinement loss of hexagonal PCF as a function of air hole diameter and external stress, where external stress  $P$ ,  $\lambda=1.55\mu\text{m}$ ,  $\Lambda=2.5\mu\text{m}$  and  $Nr=4$ .

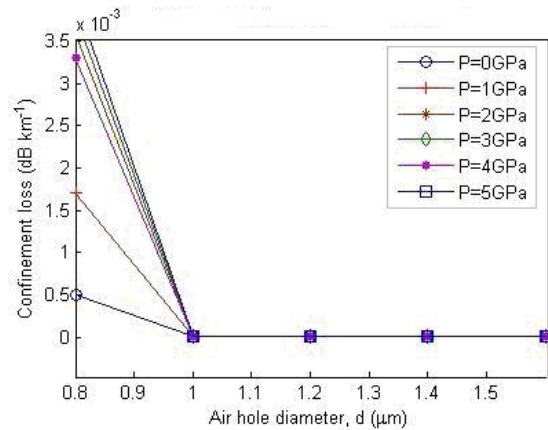
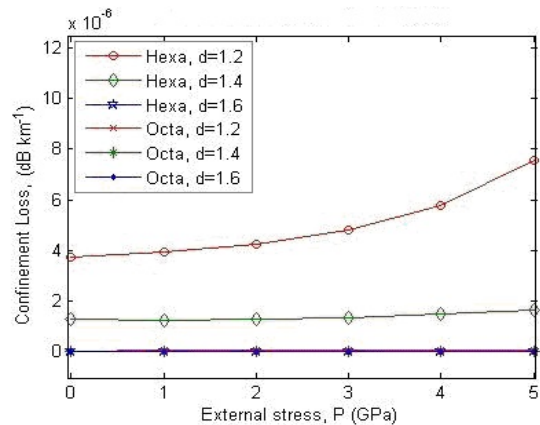


Fig.9: Confinement loss of octagonal PCF as a function of air hole diameter and external stress, where  $\lambda=1.55\mu\text{m}$ ,  $\Lambda=2.5\mu\text{m}$  and  $Nr=4$ .



(a)

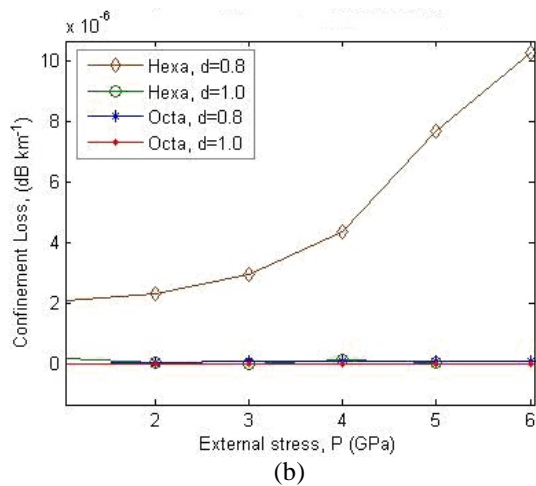


Fig.10: Confinement loss of hexagonal and octagonal PCF as a function of external stress and air hole diameter, where  $\lambda=1.55\mu\text{m}$ ,  $\Lambda=2.5\mu\text{m}$  and  $Nr=4$ .

#### 4. CONCLUSION

In this research work an analysis has been carried out to observe the effect of thermal and external stress on birefringence and confinement loss for both hexagonal and octagonal air hole arranged PCFs. It is found that the external stress induces higher birefringence for hexagonal PCFs than octagonal. It is also found that confinement loss as a function of stress increases more sharply for hexagonal PCFs. For both structures effect of stress on confinement loss is larger for smaller air diameter than larger. From our simulation result we could infer that external stress affects more on birefringence and confinement loss properties of hexagonal PCFs than octagonal and again this effect is larger for smaller air hole diameter.

#### 5. REFERENCES

- [1] K. Saitoh and M. Koshiba, "Numerical modeling of photonic crystal fibers", *Journal of Lightwave Technology*, vol. 23, no. 11, pp. 3580 – 3590, 2005.
- [2] M. Pourmahyabadi and S. M. Nejad, "Numerical analysis of index-guiding photonic crystal fibers with low confinement loss and ultra-flattened dispersion by FDFD method", *Iranian Journal of Electrical & Electronic Engineering*, vol. 5, no. 3, pp.170-197, 2009.
- [3] L. Zhao-Lun, L. Lan-Tian and W. Wei, "Tailoring nonlinearity and dispersion of photonic crystal fibers using hybrid cladding", *Brazilian Journal of Physics*, vol. 39, no. 1, pp. 50-54, 2009.
- [4] J. S. Chiang and T. L. Wu, "Analysis of propagation characteristics for an octagonal photonic crystal fiber (O-PCF)", *Optics Communications*, vol. 258, no. 2, pp. 170–176, 2006.
- [5] S. S. A. Obayya, B. M. A. Rahman and K. T. V. Grattan, "Accurate finite element modal solution of photonic crystal fibers," *IEEE Proceedings, Optoelectronics*, vol. 152, no. 5, pp. 241-246, 2005.
- [6] K. Okamoto, T. Hosaka and T. Eda, "Stress analysis of optical fibers by a finite element method,"

*IEEE Journal. Quantum Electronics*", QE-17, pp. 2123-2129, 1981.

- [7] W. C. Chew and W. H. Weedon, "A 3D perfectly matched medium from modified Maxwell's equations with stretched coordinates", *IEEE Proceedings, Photonic Technology Letter*, vol. 7, no. 13, pp. 599-604, 1994.
- [8] W. J. Bock, J. Chen, T. Eftimov and W. Urbanczyk, "A photonic crystal fiber sensor for pressure measurements," *IEEE Proceedings, Transactions on Instrumentation and Measurement*, vol. 55, no. 4, pp. 1119–1123, 2006.
- [9] M. A. Hossain and M. S. Alam, "Polarization properties of photonic crystal fibers considering thermal and external stress effects", *Proceedings of International Conference on Advanced Communication Technology*, ISSN. 1738-9445, pp. 879 – 883, 2010.
- [10] Z. Zhu and T. G. Brown, "Stress-induced birefringence in micro structured optical fibers", *Optical Letters*, vol. 28, no. 23, pp. 495 – 503, 2003.
- [11] M. Szpulak, T. Martynkien and W. Urbanczyk, "Effects of hydrostatic pressure on phase and group modal birefringence in micro-structured holey fibers", *Applied Optics Journal*, vol. 43, no. 24, pp. 4739-4744, 2004.,
- [12] H. Tian, Z. Yu, Han L. and Y. Liu, "Birefringence and confinement loss properties in photonic crystal fibers under lateral stress", *IEEE Photonic Technology. Letter*, vol. 20, no. 22, pp. 1830 – 1832, 2008.

#### 8. NOMENCLATURE

Symbol	Meaning	Unit
$n$	Refractive index	Dimensionless
$n_{eff}$	Effective index	Dimensionless
$P$	Pressure	(Pa)
$\lambda$	Wavelength	( $\mu\text{m}$ )
$\Lambda$	Pitch	( $\mu\text{m}$ )
$d$	Air hole diameter	( $\mu\text{m}$ )
$Nr$	Number of air hole rings	Dimensionless
$D$	Fiber cross section diameter	( $\mu\text{m}$ )
$e$	PML width	( $\mu\text{m}$ )